# Adaptive CNC Machining Process Optimization of Near- net- shaped Blade based on Machining Error data Flow Control

**Dongbo Wu**
Tsinghua University
**wang hui** ( wdb4451253@126.com )
Tsinghua University
**he lei**
Tsinghua University
**Jie Yu**
AECC

**Original Article**

**Keywords:** Adaptive CNC machining process, Machining error data flow, Dynamic displacement response, Near- net- shaped blade

**Posted Date:** July 7th, 2021

**DOI:** https://doi.org/10.21203/rs.3.rs-664182/v1

# Adaptive CNC machining process optimization of near- net- shaped blade based on machining error data flow control

Dongbo Wu [1], Hui Wang [1 *], He Lei [1], Jie Yu [2]

[1] *State Key Laboratory of Tribology, Beijing Key Lab of Precision/Ultra-Precision Manufacturing Equipment and Control, Department of Mechanical Engineering, Tsinghua University, Beijing, China 100084, P.R. China.*

[2] *AECC Xi'an Aero-engine LTD. Xi'an, Shannxi 710021, P. R. China.*

*#Corresponding Author / E-mail: wdb4451253@126.com, TE, TEL: +86-10-62798599*

**Abstract:** Adaptive CNC machining process is one of the efficient processing solution for near- net- shaped blade, this study proposes an adaptive computer numerical control (CNC) machining process optimization scheme based on multi-process machining errors data flow control. The geometric and mechanical models of the multi-process adaptive CNC machining process are firstly constructed. The multi-process machining error data flow and the process system stiffness of near- net- shaped blade are then experimentally explored. The machining error flow collaborative control of the near-net- shaped blade multi-process CNC machining is finally realized by the adaptive CNC machining process under the premise of sufficient stiffness of the blade- fixture system. The results show that the dynamic displacement response of the blade multi-process CNC machining process is controlled within 0.007mm. The optimized adaptive CNC machining process based on the multi-process geometric machining error data flow control and the sufficient stiffness of blade- fixture system can realize the multi-process machining error control and high-precision machining of near- net- shaped blade. The process chain of the optimized adaptive CNC machining process is reduced by 87% compared with the low melting point alloy pouring process and 50% compared with adaptive CNC machining process of the twice on-machine measurement on the blade body.

**Keywords:** Adaptive CNC machining process, Machining error data flow, Dynamic displacement response, Near- net- shaped blade.

# 1 Introduction

Blade, as one of the most used functional part in aero-engine, is the key part for the realization and improvement of aero-engine performance. Near- net- shaped blade, such as precision-forged blades without margins, precision-cast blades without margins, will be the future development trend due to the complex curved surface of near- net- shaped blade is directly formed by the forming process without the material removal link on the blade surface, which can improve the blade body anti-fatigue performance under the high temperature, high pressure and high speed conditions [1].

Figure 1 is a typical near- net- shaped blade formed by the precision forging forming process, the contour error of the blade body is in the range of 0.008mm to 0.05mm, which meets the accuracy requirements of the blade body and does not require subsequent CNC machining process. However, the subsequent CNC machining process of the blade leading and trailing edges (LTE), tenon root and tip is indispensable due to the small radius curvature and high precision requirement [2]. In the CNC machining process of the blade LTE, tenon root and tip, the only available positioning surface is the blade body profile. However, the formed blade body profile has an initial contour error of 0.008- 0.05mm. The clamping surface is only the blade body which is a 5mm thick blade. The high processing requirements which the contour error of the tenon root is less than 0.007 mm, the roughness is less than Ra 0.8 um, and the section torsion is less than 0.15 degree should be finally completed by CNC machining process. Therefore, the machining error control and stiffness improvement are the key challenge for near- net- shaped blade CNC machining process.

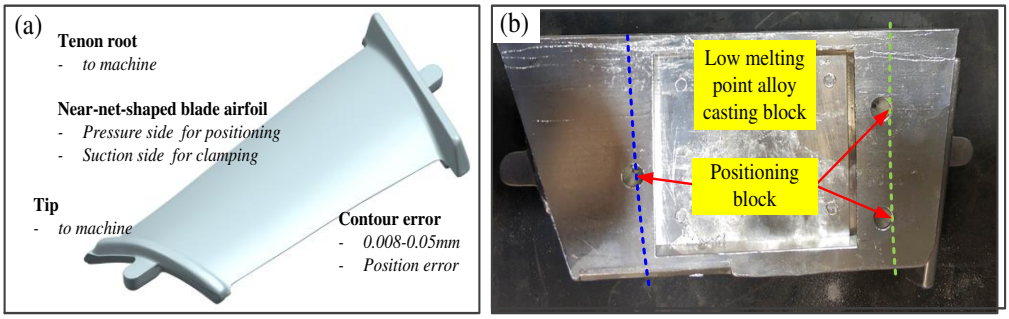


**Fig. 1** Near- net- shaped blade and the low melting point alloy pouring process, (a) near- net- shaped blade blank, (b) the low melting point alloy pouring process

The existing CNC machining process for this near- net- shaped blade is a low-melting-point alloy casting method in which the blade is poured into a block through the low-melting-point alloy to improve the stiffness of the process system. There are 15 process procedures in the mechanical processing stage (see Figure 2). However, the

disadvantages of the low surface positioning accuracy, long process chain, and blade surface alloy contamination make it is difficult to meet the performance requirements of the new generation aero-engine.

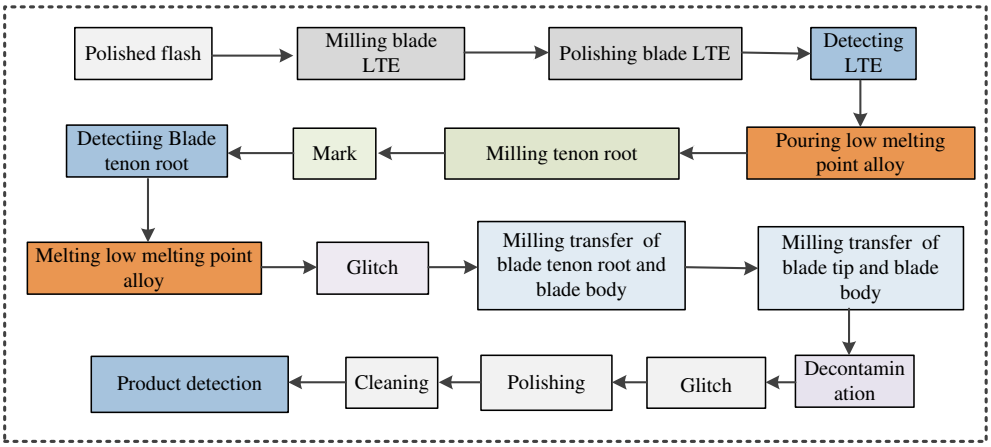


**Fig. 2** The process flow of low melting point alloy pouring process

There are many studies for the CNC machining process of near- net- shaped blade, which mainly considered from two aspects, one is the machining error control during the multi-process machining process, and the other is the stiffness improvement of the process system.

The multi-process machining error transmission is not conducive to machining accuracy improvement of the blade, this is because that machining error are accumulated in space domain and transmitted in the time domain. The machining errors transmission control of the multi-process will be the key to improve the machining quality of near- net- shaped blade. SJ Hu et al [3]. proposed a theoretical method for the error flow of mechanical product assembly based on the error transmission characteristics of multiple parts. D. Ceglarek et al [4, 5]. further developed the state-space equation method to study assembly error variation relationship modeling and deviation transmission mechanism. Walid Ghiea et al [6]. calculated the error transfer based on the Jacobian matrix based on small displacement torsor (SDT). Rong et al. [7] comprehensively explained the influence of positioning error on the machining accuracy, and established a complete geometric positioning error calculation and sensitive factor analysis model. Mantripragada et al. [8] proposed a state transition model for the deviation transfer of a multi-process manufacturing system. Therefore, the method of error data stream transmitting can be used to solve the multi-process machining error control of near- net- shaped blade, which will be a research way to optimize the CNC machining process.

There are also many studies on the stiffness improvement of the process system.

Jiayuan He et al. [9] used the finite element method (FEM) to optimize the fixture positioning layout to enhance the stiffness of thin-walled parts and reduce the deformation error in CNC machining process. Asante et al. [10] predicted the pressure distribution based on the contact modeling and finite element methods to optimize the clamping force to increase the stiffness of the process system. Wang Ying et al. [11, 12] established a part stiffness analysis model by finite element method, and then discussed the correlation between positioning errors, deformation errors and machining errors. K.P. Padmanaban et al. [13] proposed a method to optimize the fixture layout through the ant colony optimization algorithm to control the elastic deformation of part. He Ning et al. [14] paid more attention to the elastic deformation of parts under the cutting motion of the cutter and the corresponding surface machining error. Chen Weifang et al. [15] proposed a multi-objective optimization method based on genetic algorithm to improve the stiffness of the process system and reduce deformation. E. Budak et al. [16] studied the cutting force, structural deformation and surface accuracy during the cutting process of workpieces. Wu Baohai et al. [17- 19] analyzed the cutting force model and the dynamic characteristics of the blade and blisk, which showed that the stiffness of the weak rigid system affected the machined surface. Calleja, A et al. [20, 21] studied the highly accurate 5-axis flank CNC machining with conical tools, and analyzed blisk blades manufactured strategies by different manufacturing process to determine optimal machining process for blisk manufactured in low machinability materials. Zhang, Y. et al. [22] presented a 5-axis adaptive machining framework for the LE/TE of near-net-shape integrated impeller, and the on-machine measurement (OMM) with a touch-trigger probe was utilized to digitalize the impeller, which provides solutions for high-quality processing of impeller. Feng Yazhou. et al. [22] studied the precision forged blade adaptive processing model reconstruction algorithm, including measurement point selection, measurement path planning and processing model reconstruction. Liu Xuan . et al. [23] studied adaptive machining model matching technology for hollow blade, and achieved the high-precision manufacturing of hollow blade based on adaptive processing technology. Tian Weijun. et al. [24] studied the chatter suppression method for multi-axis machining of thin-walled blades, and improveds the processing quality of blade through vibration suppression technology. Lu Yaoan. et al. [25] studied the tool path generation method of five-axis wide-row machining process, and improved machining quality through machining path optimization. Li-Min Zhou et al. [26, 27] proposed a method for predicting the surface dimensional form errors caused

by deflections of both the workpiece and the slender end-mill in the five-axis flank milling of thin-walled parts, and the machining accuracy was improved through deformation prediction during the CNC machining process for the case of the insufficient stiffness of thin-walled parts.

In summary, in order to achieve high-precision machining of near- net- shaped blade, the adaptive CNC machining process should be optimized from the stiffness improvement and machining error control. The structure of this study is arranged as follows. The multi-process adaptive CNC machining process of near- net- shaped blade is studied based on theoretical method in section 2. The experimental conditions and methods for adaptive CNC machining process optimization and dynamic performance testing are shown in Section 3. Experimental results and discussion are in Section 4. The conclusion is summarized in section 5.

## 2 Theory of the multi-process adaptive CNC machining process

Adaptive CNC machining process is the solution of the high accuracy machining of near- net- shaped blade tenon root, tip and LTE, and this method is mainly based on the idea of closed-loop optimization iteration, and on-machine measurement of the spatial pose and shape of the blade, adaptive adjustment of the processing scheme and tool trajectory to improve blade machining accuracy.

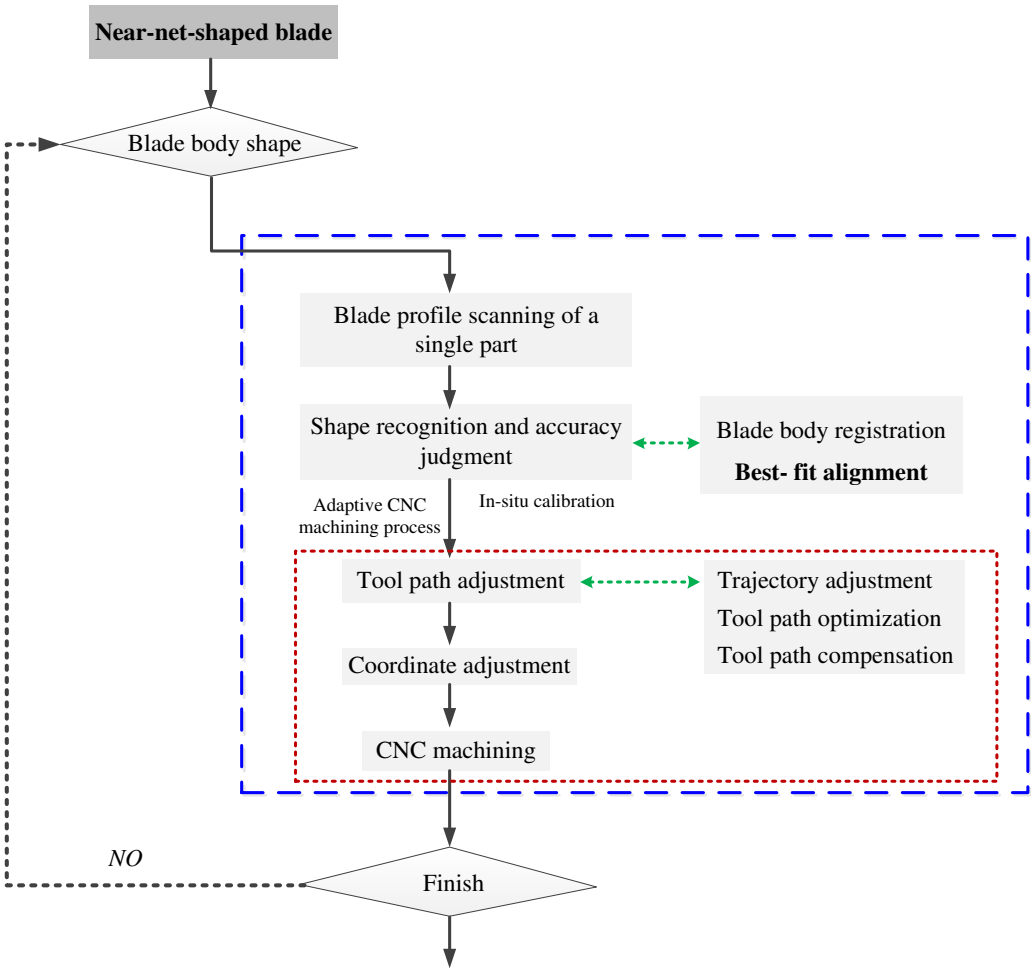


**Fig. 3** The process flow of adaptive CNC machining process

Figure 3 is the process flow of adaptive CNC machining process for near- net-shaped blade. The profile characteristic of each blade is firstly measured due to the contour accuracy of each near- net- shaped blade is inconsistent. The tool path adjustment matrix is then accurately calculated based on the measurement points and theoretical points by adaptive CNC machining process algorithm. The tool path adjustment, coordinate adjustment or blade pose transformation are finally obtained to achieve high accuracy CNC machining of near- net- shaped blade.

For a specific near- net- shaped blade, the spline curve is used to generate the blade body curve, the parametric equation of this spline curve can be obtained if the curve control points are known.

$$\mathbf{C}(u)=\frac{\sum_{i=0}^{n}N_{i,p}(u)\omega_i P_i}{\sum_{i=0}^{n}N_{i,p}(u)\omega_i},a<u<b \tag{1}$$

where $P_i$ is control point, $\omega_i$ is weight factor associated with the $P_i$, and $\omega_i>0$, $N_{i,p}(u)$ is

a 3-order normative B-spline basis function defined on the non-uniform node

In order to obtain the parametric equation of this B-spline curve, the curve control points need to be obtained.

$$U = \{\underbrace{0,0,0}_{p+1}, u_{p+1}, \ldots, u_{r-p-1}, \underbrace{1,1,1}_{p+1}\} \tag{2}$$

A one-element basis function can be introduced if the control points of the blade section line are known.

$$R_{i,p}(u) = \frac{N_{i,p}(u)\omega_i}{\sum_{j=0}^{n} N_{j,p}(u)\omega_j} \tag{3}$$

The blade curve equation is generated as the Formula (4)

$$\mathbf{C}(u) = \sum_{i=0}^{n} R_{i,p}(u) P_i \tag{4}$$

where $R_{i,p}(u)$ is the piecewise rational basis function defined on the interval $u \in [0,1]$.

In fact, if the measurement points in the actual state are obtained as the spline control points, the measurement model will be obtained according to Formula (1) to (4), and the theoretical model corresponding to the measurement model can also be obtained. Therefore, what needs to be calculated in adaptive CNC machining process is the matrix relationship between the measurement points and the theoretical points, and can be obtained by the registration algorithm.

The registration principle is the least square method, and its essence is to obtain the minimum distance between the theoretical points and the measurement points, and obtain the rotation and translation matrix based on this minimum distance.

$$F = \min \sum_{i=1}^{n} d_i^{\,2} = \min \sum_{i=1}^{n} \left[\text{distance}(p_i, q_i)\right]^2 \tag{5}$$

where $P_i$ is the measurement point, and $q_i$ is the theoretical point, $F$ is the target parameter of registration and is distance value in this registration.

The rotation matrix is shown in Formula (6)

$$R = \begin{bmatrix} \cos\beta\cos\gamma & \cos\beta\sin\gamma & -\sin\beta \\ \sin\alpha\sin\beta\cos\gamma - \cos\alpha\sin\gamma & \sin\alpha\sin\beta\sin\gamma - \cos\alpha\cos\gamma & \sin\alpha\cos\beta \\ \cos\alpha\sin\beta\cos\gamma + \sin\alpha\cos\gamma & \cos\alpha\sin\beta\sin\gamma - \sin\alpha\cos\gamma & \cos\alpha\cos\beta \end{bmatrix} \tag{6}$$

where $\alpha$ is the rotation angle of the blade along with the machine tool's $A$ axis, $\beta$ is the rotation angle of the blade along with the machine tool's $B$ axis, and $r$ is the rotation angle of the blade along with the machine tool's $C$ axis.

The translation matrix is shown in Formula (7)

$$T = [T_x \;\; T_y \;\; T_z]^T \tag{7}$$

where, $T$ is the blade translation matrix, $T_x$ is the blade translation along with the machine tool's $x$ axis, $T_y$ is the blade translation along with the machine tool's $y$ axis, and $T_z$ is the blade translation along with machine tool's the $z$ axis.

The above Formulas of (1) to (7) are the geometric flow of the blade adaptive CNC machining process. The position and posture of the blade after clamping can be adjusted based on the above adaptive CNC machining process, and the blade deformation caused by the cutting force can also be adjusted based on the above adaptive CNC machining process. However, the blade deformation caused by the cutting force is a dynamic displacement response due to the cutting force is a dynamically changing time-varying force, and the real-time position and posture adjustment during the cutting process will break the continuity of cutting process, and the interrupt of the cutting process will cause the existence of tool marks, which will seriously affect the quality of blade. On the other hand, the real-time position and posture adjustment will also reduce the efficiency of blade CNC machining process. The dynamic response value of the blade during cutting processing is small if the stiffness of the blade process system is adequate, and the adaptive CNC machining process will have good efficiency and processing accuracy. Therefore, the sufficient stiffness of the blade process system and small dynamic displacement response are the prerequisite for the optimization of the adaptive CNC machining process.

In CNC machining process, the blade and fixture are the stiffness weak link in the process system relative to machine tools and cutter, and the blade- fixture system should have the sufficient capacity to suppress the blade deformation and vibration due to the blade is typical thin-walled part.

The blade deformation under the clamping force and cutting force is shown in Formula (8)

$$\frac{\partial^4 w}{\partial x^4} + 2\frac{\partial^4 w}{\partial x^2 \partial y^2} + \frac{\partial^4 w}{\partial y^4} = \frac{1}{D}\left(p(x) + \sigma_x \frac{\partial^2 w}{\partial x^2} + 2\tau_{xy}\frac{\partial^2 w}{\partial x\, \partial y} + \sigma_y \frac{\partial^2 w}{\partial y^2}\right) \tag{8}$$

The dynamic equation of the blade- fixture system during the CNC machining process is shown in Formula (9).

$$m\ddot{x}(t) + c\dot{x}(t) + kx(t) = f(t) + P\cos\omega_0 t \tag{9}$$

where $m$ is the modal mass, $c$ is the modal damping, $k$ is the modal stiffness, $f(t)$ is the

self-excited force, and $P\cos\omega_0 t$ is the harmonic force, where the frequency is $\omega_0$, and the amplitude is $P$, and $x(t)$ is the vibrational displacement between the cutter and the blade.

The forced vibration caused by the cyclic cutting force and the displacement response caused by the forced vibration will be copied on the blade surface, which will change the cutting depth of the blade, and this change cannot be adjusted by the adaptive CNC machining process. Therefore, the stiffness and damping of the blade- fixture system have a great influence on the dynamic behavior in the dynamic equation of the blade and is also a prerequisite for blade adaptive CNC machining process optimization.

## 3 Conditions and methods

The CNC machining process of near- net- shaped blade mainly includes three process procedures, the first process procedure is the CNC machining process of blade LTE, and the second process procedure is the CNC machining process of blade tenon root and tip, and the third process procedure is the detection process of the contour error of the blade tenon root and the position error of blade tenon root which is relative to the blade body.

In order to achieve high precision CNC machining of near- net- shaped blade, the experiment is mainly considered from two aspects, one is to improve the stiffness of the blade- fixture system, and the another is to optimize the adaptive CNC machining process based on the multi- process machining error data flow control, and the sufficient stiffness of blade- fixture system is the prerequisite condition for the subsequent adaptive CNC machining process optimization. The experiment method of the blade-fixture system stiffness includes the natural frequency test of the blade- fixture system and the dynamic displacement response test of blade during the CNC machining process. The experiment of adaptive CNC machining process optimization includes the test of machining errors in multiple- process of near- net- shaped blade. The experimental steps are as follows.

**Step 1**: Natural frequency test of the multi-process blade- fixture system. The acceleration sensor (Dytran 3225M23) is used to measure response curve of blade-fixture system excited by the force hammer (Dytran 5850B), the LMS data-acquisition system is used to collect the displacement response signal of the blade-fixture system from the acceleration sensor.

Figure 4 is the natural frequency test platform of the first process procedure of CNC machining process of near- net- shaped blade. The natural frequency of blade in

the cantilever beam state is firstly tested (see Figure 4 (a)), and the natural frequency of blade in the simply supported beam state restricted by machine tool top is then tested (see Figure 4 (b)). Finally, a reasonable clamping plan is obtained through comparative analysis to improve the stiffness of the blade- fixture system.

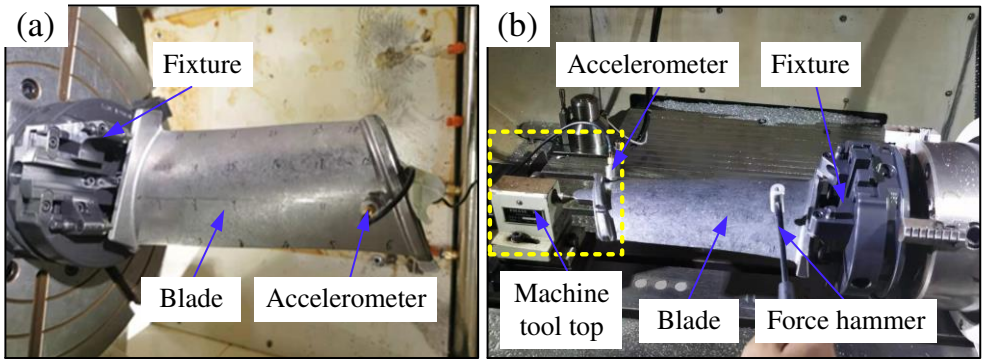


**Fig. 4** Natural frequency test platform of blade- fixture system in the first process sequence, (a) in the cantilever beam state, (b) in the simply supported beam state.

Figure 5 is the natural frequency test platform of the second process procedure of CNC machining process of near- net- shaped blade, and fixture 1# is designed and manufactured through fixture material and structural layout optimization [28], and fixture 2# is used as a comparative experiment, and the blade is the same blade, and the only variable is the machining fixture.

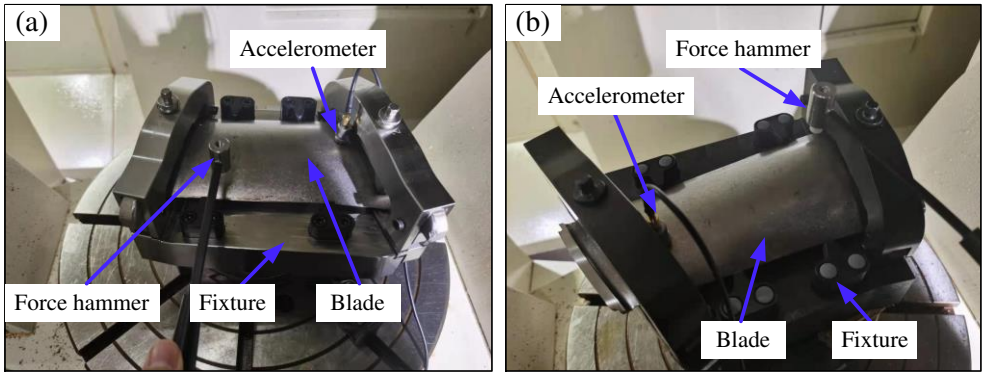


**Fig. 5** Natural frequency test platform of blade- fixture system in the second process sequence, (a) fixture 1#, (b) fixture 2#

**Step 2**: Dynamic displacement response test of multi-process blade- fixture system. Figure 6 is the dynamic displacement response test platform, and the laser displacement sensor is used to obtain the blade dynamic displacement response under the action of cutting force, and the sensitivity of the laser displacement sensor is 0.001mm, and the measurement frequency is 1024 Hz to ensure that the blade dynamic displacement response under the dynamic cutting force is tracked. The acceleration sensor is used to measure the vibration characteristic of the blade during cutting process, and the

dynamic displacement response of the blade during the cutting process can be analyzed by frequency domain analysis and time domain analysis of the vibration signal obtained by the vibration acceleration sensor and the dynamic displacement signal obtained by the laser displacement sensor.

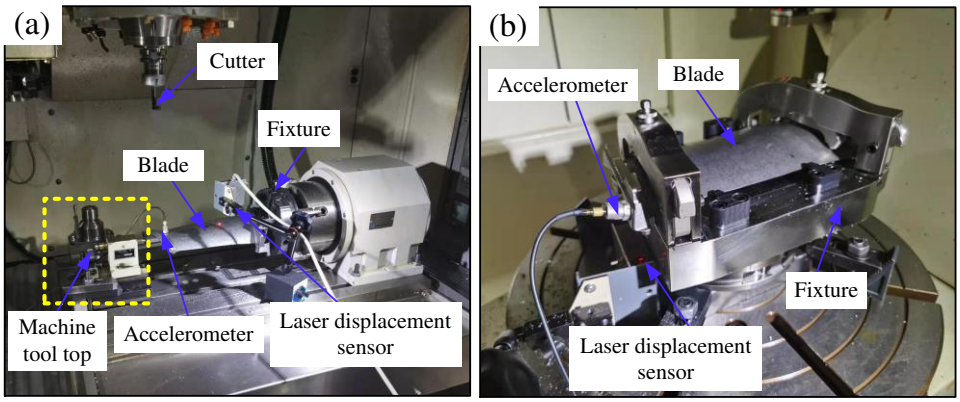


**Fig. 6** Dynamic displacement response test platform, (a) the first process sequence, (b) the second process sequence

**Step 3**: Experimental test of multi-process adaptive CNC machining process optimization based on machining error data flow control, a four- axis and five-axis CNC machine tool with integrated Renishaw probe is used in this experiment, and the Renishaw probe will be stored in the cutter magazine of machine tool, and the cutter and Renishaw probe can be switched in order by the cutter change system of machine tool.

## 4 Results and discussion

### 4.1 Analysis of the natural frequency of the blade- fixture system

Table 1 is the experiment result of the first-order natural frequency of the blade- fixture system of the first process sequence. It can be seen that the first-order natural frequency of the blade- fixture system is 121.8Hz in the cantilever beam state, and the first-order state damping ratio of the blade- fixture system is 0.3%, and the corresponding first-order mode shape is shown in Figure 7 (a). The first-order natural frequency of the blade- fixture system is 400.1Hz in the simply supported beam state which is under the constraint of the machine tool top, and the corresponding first-order damping ratio is 0.84%, and the corresponding first-order mode shape is shown in Figure 8 (a). The stiffness of the blade- fixture system is increased by 228%, and the damping ratio is increased by 180% under the simply supported beam state. The stiffness of the blade-fixture system under the constraint state of the machine tool top are greatly enhanced.

**Table 1** Natural frequency of blade- fixture system under different constraints

| Number | Constraint status 1# In the cantilever beam state Without machine tool top | | Constraint status 2# In the simply supported beam state With machine tool top | |
|---|---|---|---|---|
| | Frequency (Hz) | Damping ratio (%) | Frequency (Hz) | Damping ratio (%) |
| 1 | 121.8Hz | 0.3% | 400.1 Hz | 0.84% |
| 2 | 354.1Hz | 0.73% | 537.6Hz | 0.96% |
| 3 | 435Hz | 2.8% | 1222.6Hz | 1.86% |
| 4 | 825.7 Hz | 0.62% | 1372.8Hz | 1.4% |
| 5 | 1323.6 Hz | 0.52% | 2295.1Hz | 1.18% |

The second-order natural frequency of the blade- fixture system is 354.1Hz in the cantilever beam state, and the second-order state damping ratio of the blade- fixture system is 0.73%, and the corresponding second-order mode shape is shown in Figure 7 (b). The second-order natural frequency of the blade- fixture system is 537.6Hz in the simply supported beam state which is under the constraint of the machine tool top, and the corresponding second-order damping ratio is 0.96%, and the corresponding second-order mode shape is shown in Figure 8 (b). The stiffness of the blade- fixture system is increased by 51.8%, and the damping ratio is increased by 31.5% under the simply supported beam state. The stiffness of the blade- fixture system under the constraint state of the machine tool top are greatly enhanced.

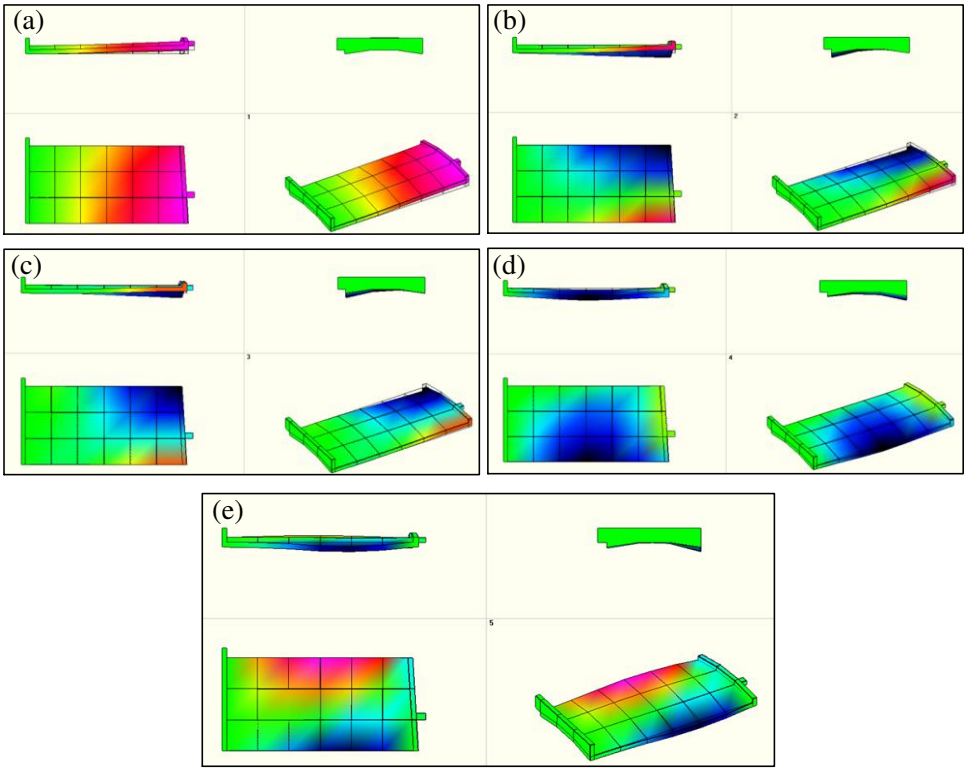


**Fig. 7** The mode shape of blade- fixture system of the first process sequence in the cantilever beam state without machine tool top, (a) the first-order mode shape, (b) the second-order mode shape, (c) the third-order mode shape, (d) the fourth-order mode shape, (e) the fifth-order mode shape.

Similarly, it can be seen that the third-order natural frequency of the blade- fixture system is increased by 181% and the damping ratio is reduced by 33% under the constraint state of the machine tool top. The fourth-order natural frequency of the blade-fixture system under the constraint state of the machine tool top is increased by 66%, and the damping ratio is increased by 125%. The fifth-order natural frequency of the system under the constraint state of the machine tool top is increased by 73%, and the damping ratio is increased by 126%. Therefore, the stiffness of the blade- fixture system in the first process procedure is greatly enhanced under the constraints of the machine tool top, which will lead to a good dynamic characteristic.

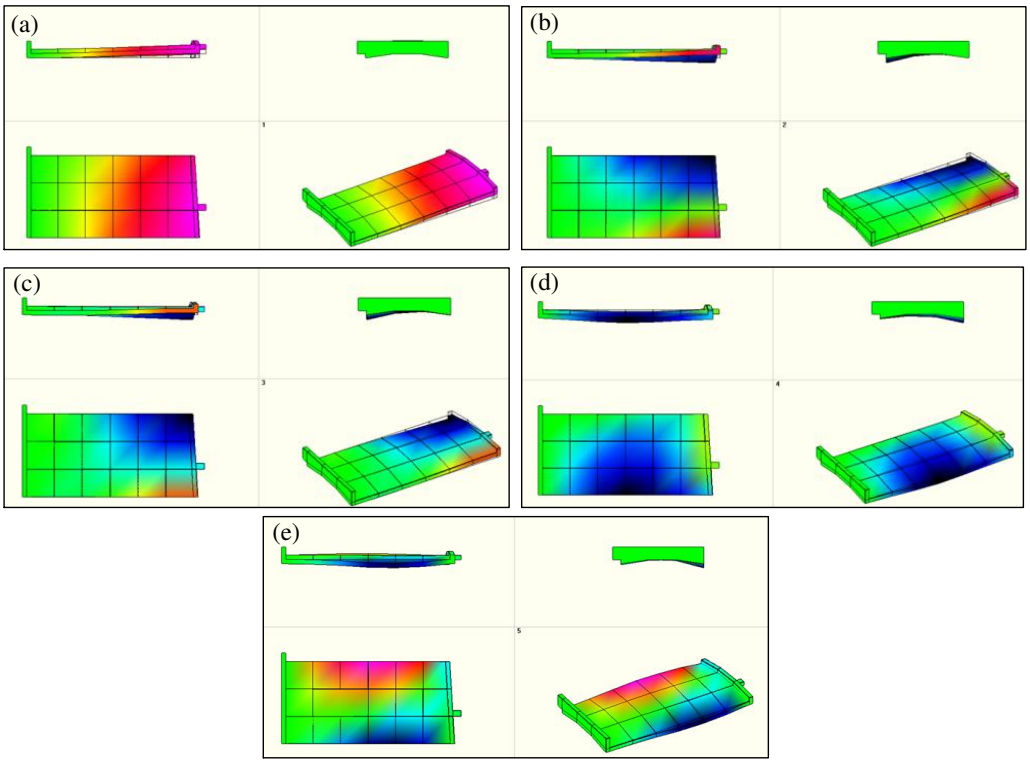


**Fig. 8** The mode shape of blade- fixture system of the first process sequence in the simply supported beam state with machine tool top, (a) the first-order mode shape, (b) the second-order mode shape, (c) the third-order mode shape, (d) the fourth-order mode shape, (e) the fifth-order mode shape.

Table 2 is the experiment result of the natural frequency of the blade- fixture system of the second processing procedure. It can be seen that the first-order natural frequency of the blade- fixture 1# system is 1105.5Hz, and the first-order damping ratio of the blade- fixture1# system is 1.78%, and the corresponding mode shape is shown in Figure 9 (a). The first-order natural frequency of the blade- fixture 2# system is 1040.7 Hz, and the first-order damping ratio of the blade- fixture 2# system is 1.97%, and the corresponding mode shape is shown in Figure 10 (a). The first-order natural frequency of the blade- fixture 2# system is increased by 5%, and the first-order damping ratio is reduced by 8% relative to the blade- fixture 1# system.

**Table 2** Natural frequency of blade- fixture system of the second processing procedure

| Number | Fixture 1# | | Fixture 2# | |
|---|---|---|---|---|
| | Frequency (Hz) | Damping ratio (%) | Frequency (Hz) | Damping ratio (%) |
| 1 | 1105.5 | 1.78 | 1040.7 | 1.94 |

| | | | | |
|---|---|---|---|---|
| 2 | 1704.8 | 0.475 | 1684 | 1.15 |
| 3 | 2385.3 | 1.4 | 2384.9 | 1.664 |

It can be seen that the first-order natural frequency of the blade- fixture 1# system is 1105.5Hz, and the first-order damping ratio of the blade- fixture 1# system is 1.78%, and the corresponding mode shape is shown in Figure 9 (a). The first-order natural frequency of the blade- fixture 2# system is 1040.7 Hz, and the first-order damping ratio of the blade- fixture 2# system is 1.97%, and the corresponding mode shape is shown in Figure 10 (a). The first-order natural frequency of the blade- fixture 2# system is increased by 5%, and the first-order damping ratio is reduced by 8% relative to the blade- fixture 1# system.

Similarly, it can be seen that the second -order natural frequency of the blade-fixture system 2# is increased by 1%, and the second -order damping ratio is increases by 13% relative to the blade- fixture 1# system, and the third -order natural frequency of the blade- fixture system 2# is increased by 0.1%, and the third -order damping ratio is increases by 18% relative to the blade- fixture 1# system. Therefore, the stiffness of the blade- fixture 1# system in the second process procedure has the good dynamic characteristics than the blade- fixture 2# system.

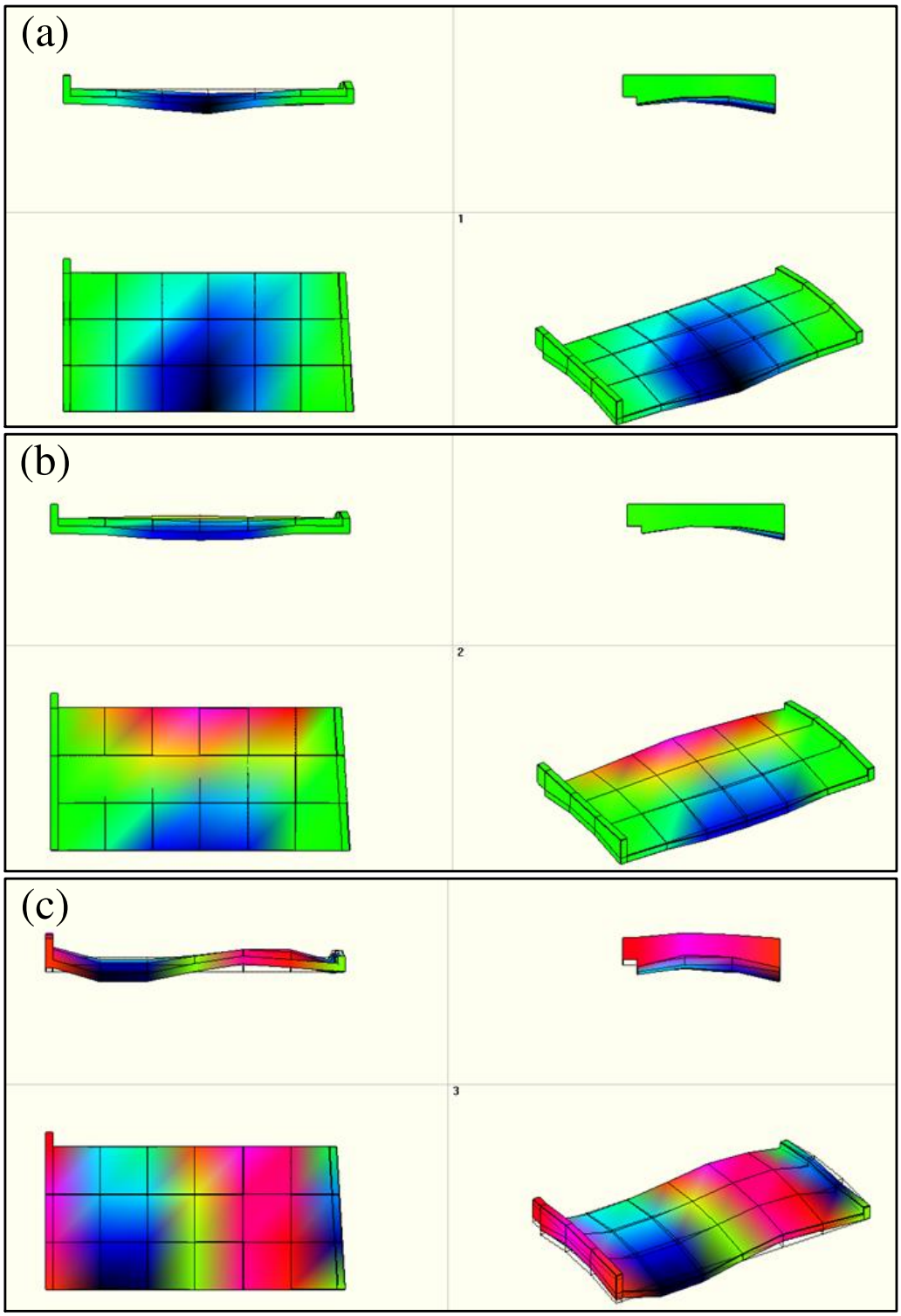


**Fig. 9** Mode shape of blade- fixture 1# system of the second process sequence, (a) the first-order mode shape, (b) the second-order mode shape, (c) the third-order mode shape.

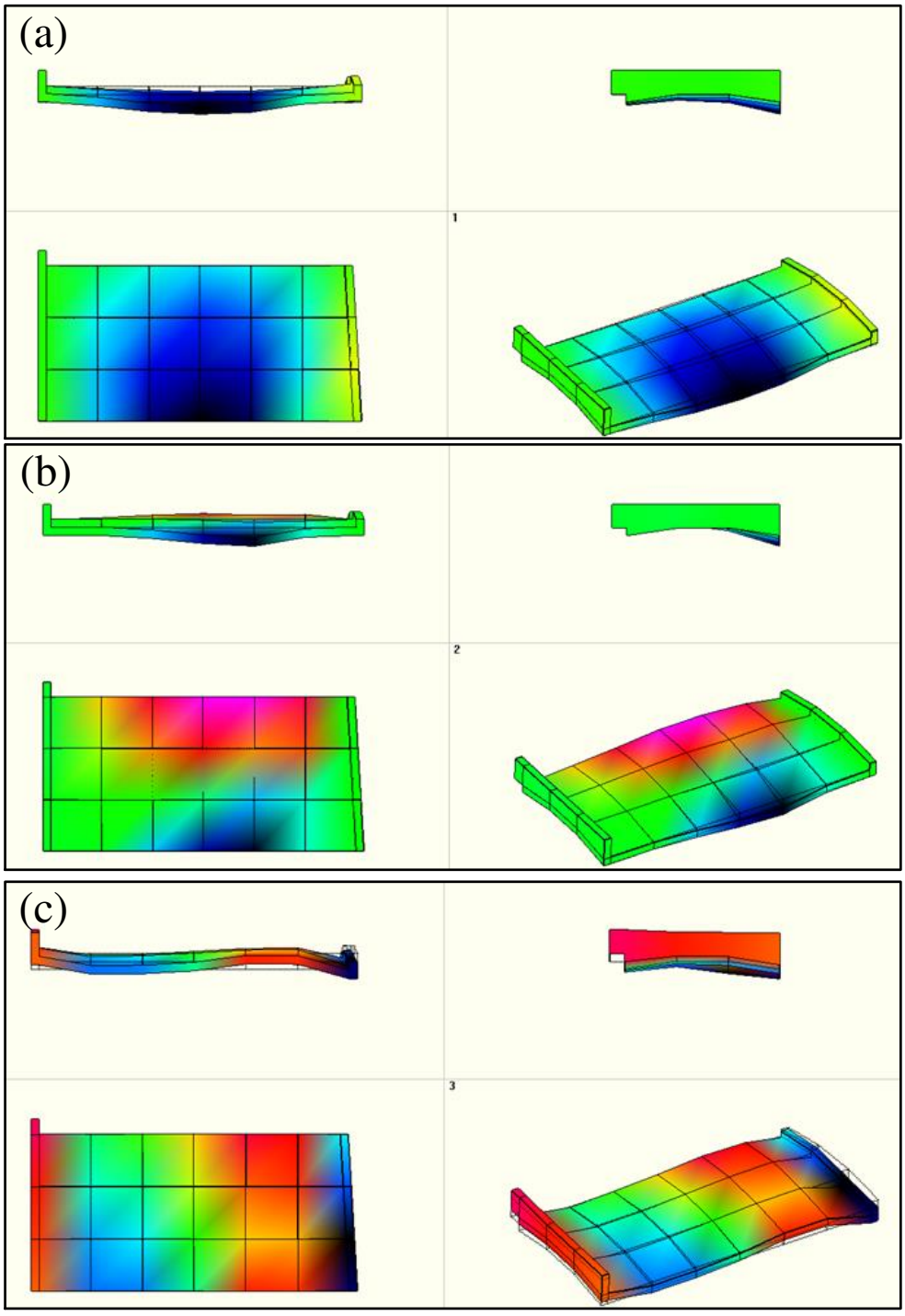


**Fig. 10** Mode shape of blade- fixture 2# system of the second process sequence, (a) the first-order mode shape, (b) the second-order mode shape, (c) the third-order mode shape.

## 4.2 Analysis of dynamic displacement response of blade

Figure 11 is the dynamic displacement response experimental result during blade CNC machining process, and Figure 11 (a) is the vibration value obtained by vibration acceleration, and Figure 11 (b) is the vibration value during one cycle of cutter force,

and Figure 11 (c) is the blade dynamic displacement response obtained by the high-precision, high-resolution laser displacement sensor, and Figure 11 (d) is the low-frequency change of the dynamic displacement response fitted by a low-pass filter.

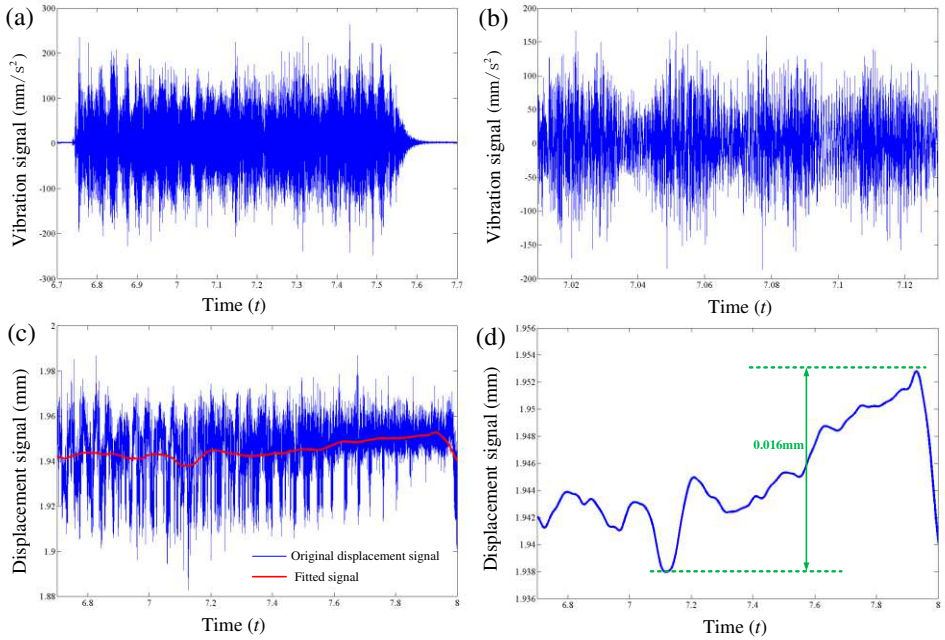


**Fig. 11** Dynamic displacement response of blade-fixture system in the first process sequence (with the machine tool top), (a) blade vibration during CNC machining process, (b) vibration value during a cycle of cutter force, (c) blade dynamic displacement response, (d) low-frequency dynamic displacement response of blade

It can be seen from Figure 11 and Figure 12 that the existence of the machine tool top greatly improves the stiffness of the blade- fixture system, and the maximum dynamic displacement response value of the blade is reduced by 1/5 under the same process parameters. The maximum dynamic displacement response value of the blade under suitable process parameters is less than 0.007mm (see Figure 13 and Table 3), the dynamic displacement response value of the blade is the instantaneous displacement change value of the blade, which is essentially the elastic deformation of the blade under the cutting force. The less dynamic displacement response value of blade means the higher stiffness of the blade- system. It can be concluded that the blade- fixture system has sufficient stiffness in the first process sequence.

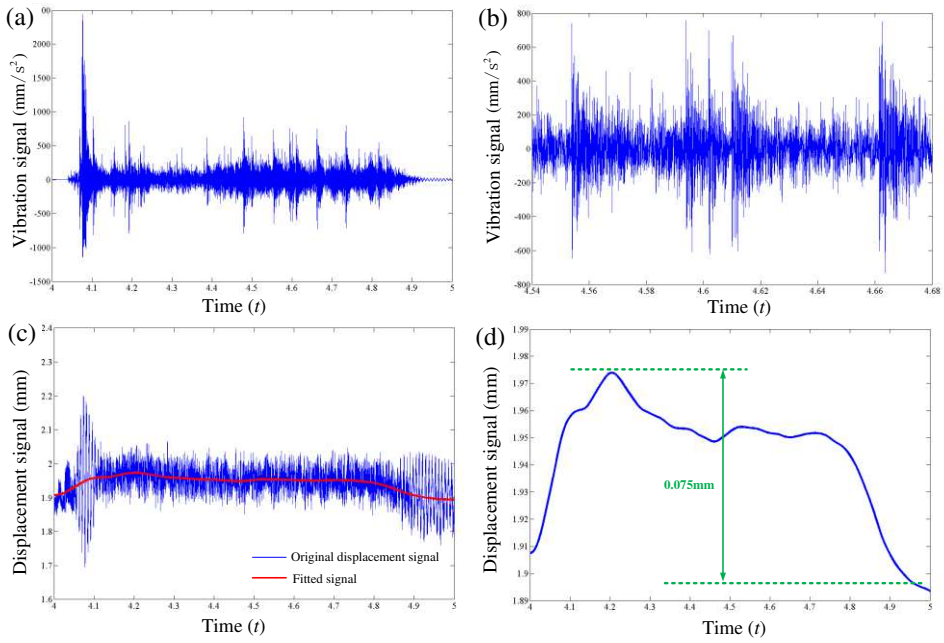


**Fig. 12** Dynamic displacement response of blade-fixture system in the first process sequence (without the machine tool top), (a) blade vibration during CNC machining process, (b) vibration value during a cycle of cutter force, (c) blade dynamic displacement response, (d) low-frequency dynamic displacement response of blade

**Table 3** The processing parameters and the maximum dynamic displacement response value of the blade in the first process sequence under the simply supported beam state with the machine tool top

| Number | Spindle speed (rpm) | Feed rate (mm/min) | Cutting depth (mm) | The maximum value of dynamic displacement response (mm) |
|---|---|---|---|---|
| 1 | 2000 | 1200 | 0.2 | 0.016 |
| 2 | 3000 | 800 | 0.2 | 0.017 |
| 3 | 3000 | 1000 | 0.2 | 0.007 |
| 4 | 3000 | 1200 | 0.1 | 0.021 |
| 5 | 3000 | 1200 | 0.2 | 0.011 |
| 6 | 3000 | 1200 | 0.3 | 0.017 |
| 7 | 3000 | 1200 | 0.05 | 0.007 |
| 8 | 3000 | 1400 | 0.2 | 0.038 |
| 9 | 4000 | 1200 | 0.2 | 0.023 |

| | | | | |
|---|---|---|---|---|
| 10 | 5000 | 1200 | 0.2 | 0.025 |

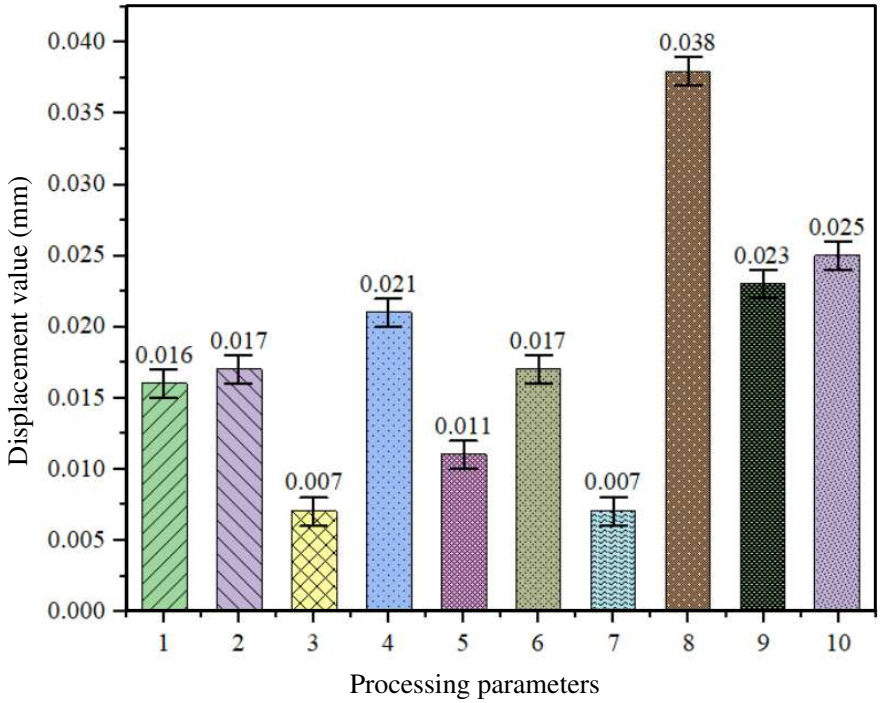


**Fig. 13** The processing parameters and the maximum dynamic displacement response value of the blade in the first process sequence under the simply supported beam state with the machine tool top

Figure 14 and Figure 15 is the dynamic displacement response experimental result during the second process sequence, and it can be seen that the proposed fixture (fixture 1#) has good dynamic characteristics to resist cutting force. The maximum dynamic displacement change value of the corresponding blade- fixture system under suitable process parameters can be controlled within 0.007mm, and the maximum dynamic displacement change value under different process parameters can still be controlled within 0.014mm (see Figure 16), which indicates that the blade- fixture system has sufficient stiffness in the second process sequence.

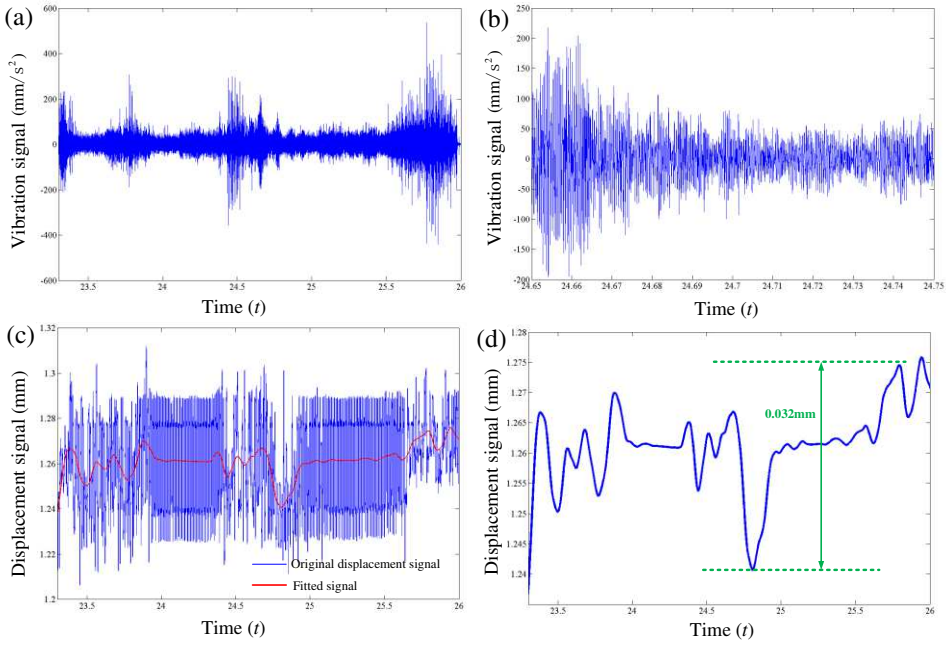


**Fig. 14** Dynamic displacement response of blade-fixture system in the second process sequence (fixture 1#), (a) blade vibration during CNC machining process, (b) vibration value during a cycle of cutter force, (c) blade dynamic displacement response, (d) low-frequency dynamic displacement response of blade

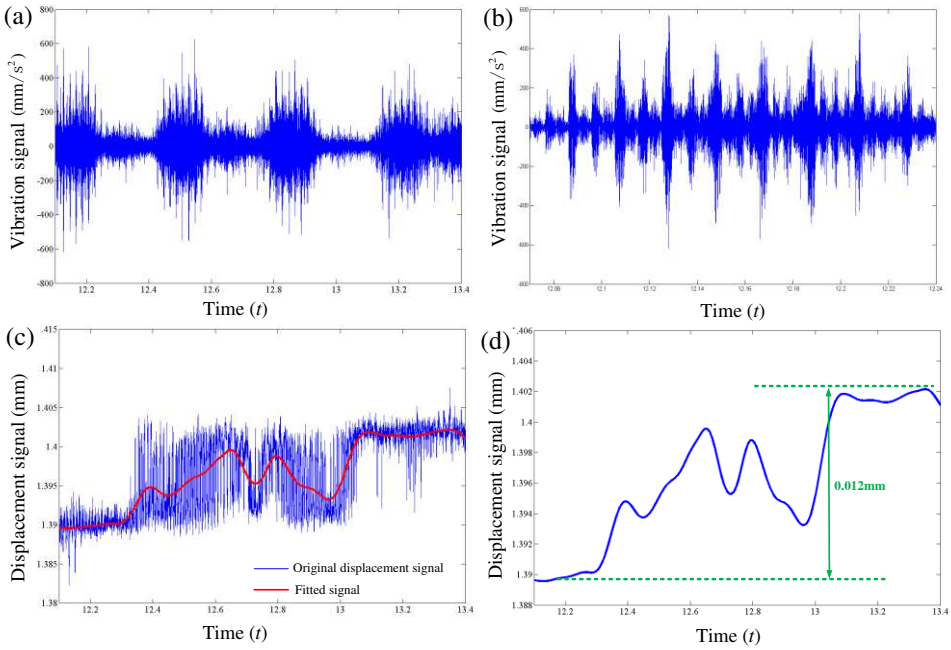


**Fig. 15** Dynamic displacement response of blade-fixture system in the second process sequence (fixture 2#), (a) blade vibration during CNC machining process, (b) vibration value during a cycle of cutter force, (c) blade dynamic displacement response, (d) low-frequency dynamic displacement response of blade

**Table 4** The processing parameters and the maximum dynamic displacement value of

blade in the second process sequence (fixture 2#)

| Number | Spindle speed (rpm) | Feed rate (mm/min) | Cutting depth (mm) | The maximum dynamic displacement value (mm) |
|---|---|---|---|---|
| 1 | 2000 | 1200 | 0.2 | 0.012 |
| 2 | 3000 | 600 | 0.2 | 0.008 |
| 3 | 3000 | 1000 | 0.2 | 0.013 |
| 4 | 3000 | 1200 | 0.1 | 0.007 |
| 5 | 3000 | 1200 | 0.2 | 0.012 |
| 6 | 3000 | 1200 | 0.3 | 0.009 |
| 7 | 3000 | 1200 | 0.4 | 0.015 |
| 8 | 3000 | 1400 | 0.2 | 0.014 |
| 9 | 4000 | 1200 | 0.2 | 0.014 |
| 10 | 5000 | 1200 | 0.2 | 0.014 |

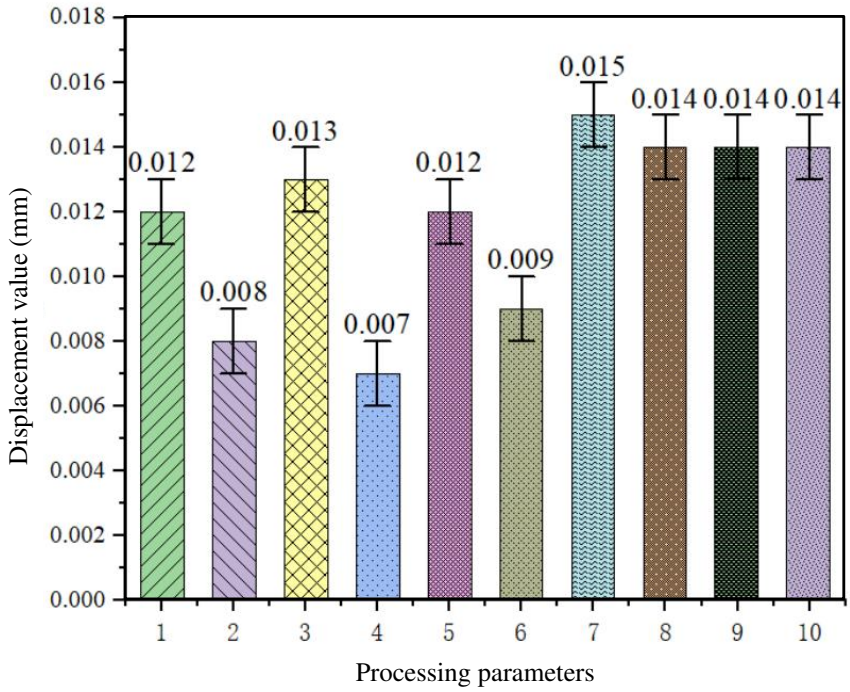


**Fig. 16** The processing parameters and the maximum dynamic displacement value of the blade in the second process sequence

In summary, it can ensure that the maximum dynamic response value of the blade is controlled within 0.007mm during blade finishing machining process and 0.015mm

during roughing machining process in the first and second process sequences, and there are no weak stiffness links in the CNC machining process considering the first and second process sequence, which provide the stiffness prerequisite condition for the optimization of the multi-process adaptive CNC machining process. The sufficient stiffness prerequisite condition combined with the adaptive CNC machining process optimization method can provide optimized solution for precision machining of near-net- shaped blade.

## 4.3 Machining error data flow control and adaptive CNC machining process optimization

Figure 17 is the machining benchmark in the CNC machining process of near- net-shaped blade, the first process sequence uses the blade false boss as the positioning benchmark to machine the blade LTE (see Figure 17 (a)), and the second process sequence uses the machined LTE and the blade body as the positioning benchmark to machine the blade tenon root and tip, and the third process sequence uses the machined blade tenon root as the benchmark to detect the position error and contour error of the blade body. It can be seen that the machining benchmark in the CNC machining process of near- net- shaped blade repeatedly changes, which will inevitably cause the accumulation and transmission of machining errors.

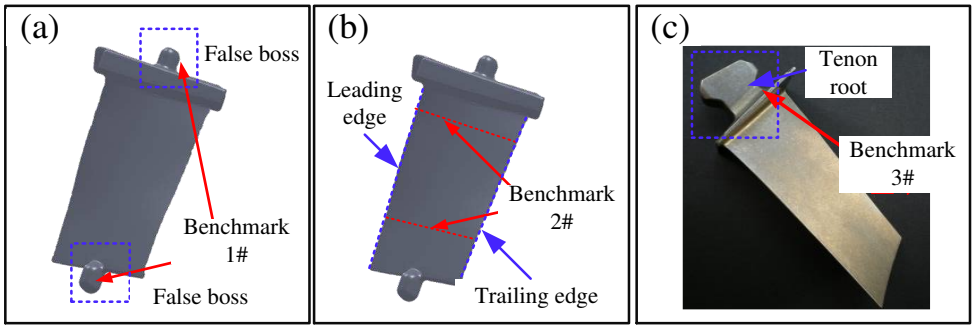


**Fig. 17** Machining benchmark in the CNC machining process of near- net- shaped blade, (a) the first process procedure benchmark, (b) the second process procedure benchmark, (c) the third process procedure benchmark.

Figure 18 is an adaptive CNC machining process scheme based on the twice blade body on-machine measurements, 81 measurement points in the blade body are firstly selected to construct measurement model to realize the adaptive CNC machining process of the blade LTE according to the data processing flow of Figure 3, and these 81 measurement points in the blade body are selected again to realize the adaptive CNC

machining process of the blade tenon root and tip. The machining efficiency and accuracy of this adaptive CNC machining process are improved compared with the low melting point alloy casting process, however, this adaptive CNC machining process is not the most efficient due to the introduction of twice blade body on-machine measurements.

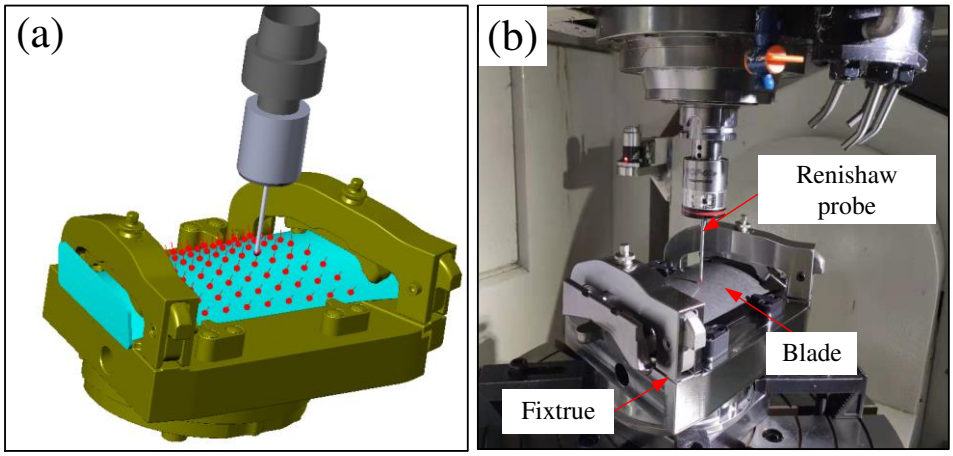


**Fig. 18** Adaptive CNC machining process based on the twice blade body on-machine measurements, (a) on-machine measurement model, (b) on-machine measurement site

It is completely possible to combine the two process procedure benchmarks as a unified benchmark from the perspective of the machining benchmark to reduce the machining errors caused by the machining benchmark conversion. If the machining benchmark facet for the second process procedure is machined at the same time in the first process procedure, the machined machining benchmark facet for the second process procedure is directly measured to reconstruct the measurement model to realize the adaptive CNC machining process of the blade tenon root and tip, and the optimized specific adaptive CNC machining process is shown in Figure 19.

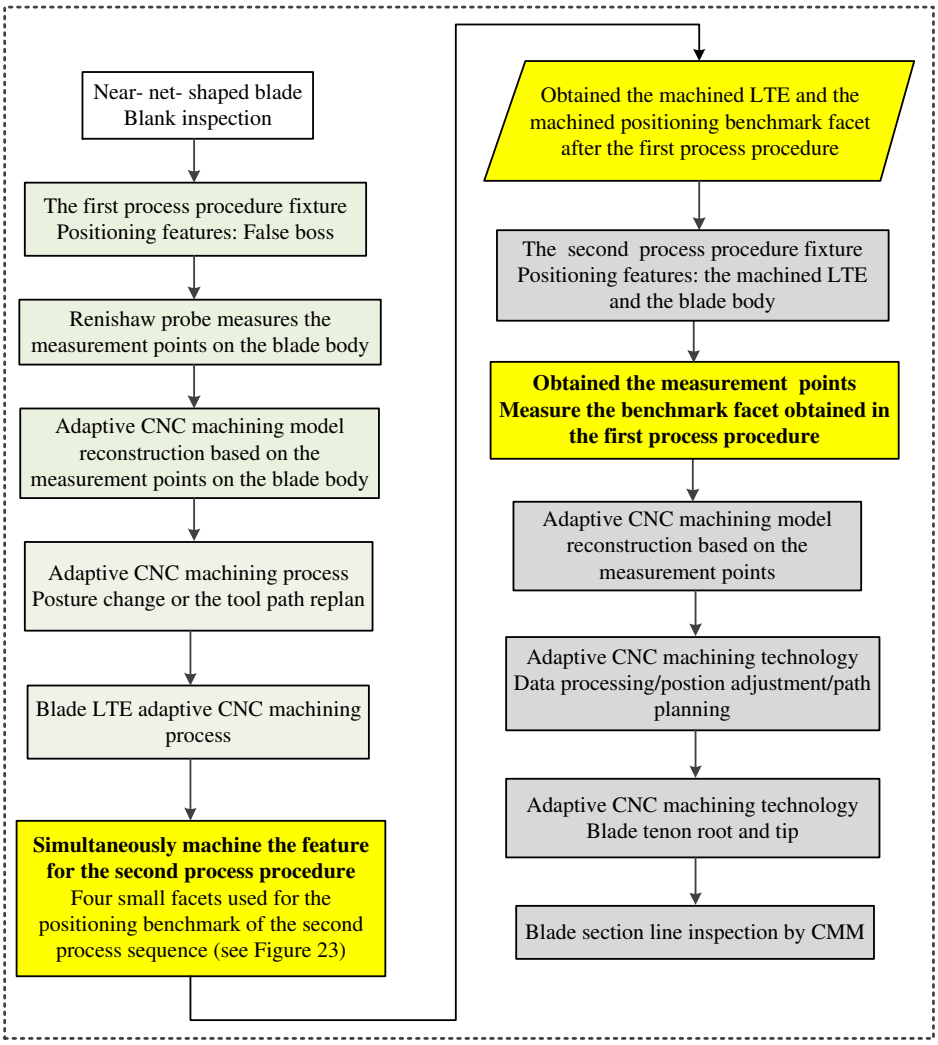


**Fig. 19** The optimized adaptive CNC machining process

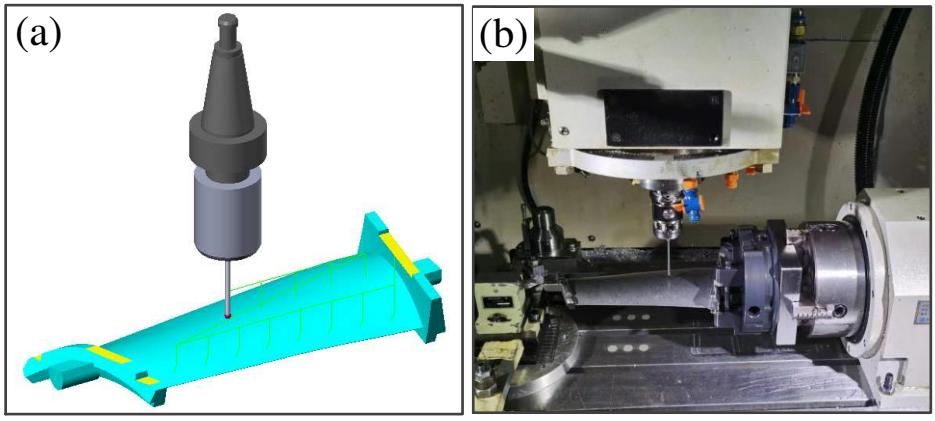


**Fig. 20** On-machine measurement of the first process sequence adaptive CNC machining process, (a) measurement points and measurement path model, (b) on-machine measurement site.

Figure 20 is on-machine measurement of the first process sequence adaptive CNC machining process, and 24 measurement points in the blade body are selected to

construct the measurement model for adaptive CNC machining process, and the measurement model and the theoretical model are registered to obtain the adaptive CNC machining process reconstruction model to ensure the position of the blade tenon root relative to the blade body.

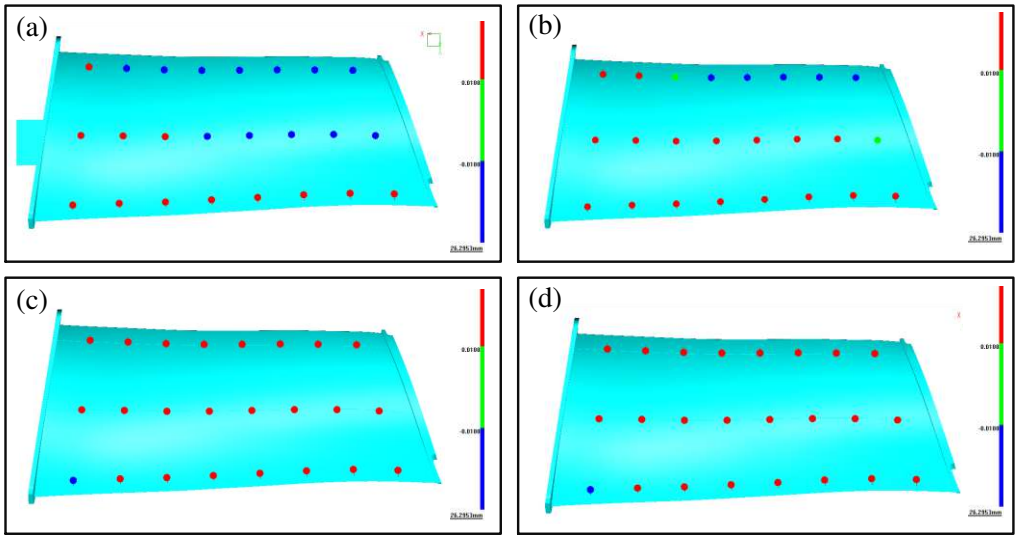


**Fig. 21** Single-point deviation value of the measurement points in the blade body, (a) the initial state of blade in the fixture, (b) adaptive CNC machining adjustment in the first stage, (c) adaptive CNC machining adjustment in the intermediate state, (d) adaptive CNC machining adjustment in the acceptable state.

Figure 21 is the single-point deviation value of the measurement points in the blade body, and it can be seen from Figure 21 (a) that some of the single-point deviation values of these 24 measurement points are greater than 0 mm, and some are less than 0 mm when the blade is initially installed on the fixture, and the specific numerical distribution is shown in Figure 22, which shows that the blade is not in the ideal position. If the blade LTE and the benchmark facet for the second process sequence are machined at this position, the machining error will be inevitably accumulated. This is because that there is a geometric deviation of 0.008- 0.05 mm in the blade body profile, and this geometric deviation values are all more than 0 mm. Therefore, it can be concluded that the blade is in an unacceptable position state when some of the single-point deviation values of these 24 measurement points are less than 0 mm, and the subsequent adaptive regulation is required, as shown in Figure 3. According to this principle, the position of the blade in Figure 21 (b) and Figure 21 (c) are all non-ideal position, however, the number of measurement points with a single point deviation value of less than 0mm is reduced comparing to Figure 21 (a), which indicates that the adaptive CNC machining process at this process plays an effective effect. The single-point deviation values of all

measurement points are greater than 0mm and uniform distribution as shown in Figure 20 (d), which shows that all measurement points of the blade body are evenly distributed on both sides of the theoretical model of the blade and the blade is in an ideal position at this time. The machining error of the blade LTE and the benchmark facet can be controlled when the blade LTE and the benchmark facet are machined in this state under the sufficient stiffness of blade- fixture system, which will provide condition for the machining benchmark transfer between the first and second process sequences.

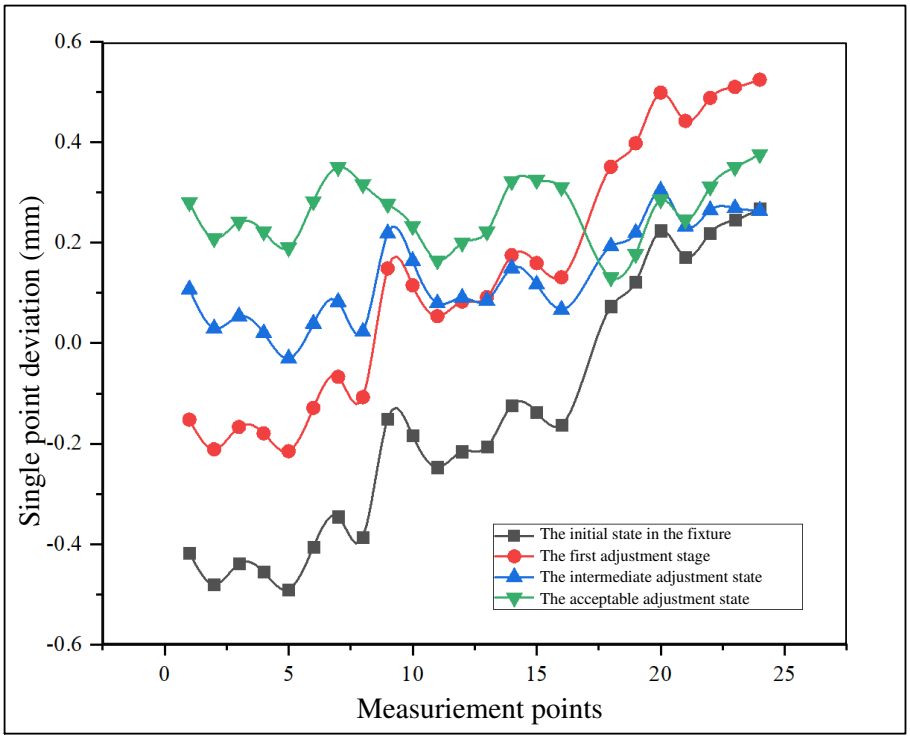


**Fig. 22** Specific numerical value distribution of single-point deviation value of blade body measurement points in the first process sequence of the adaptive CNC machining process.

Figure 23 is the machining benchmark facet for the second process sequence measurement in the four-axis machine tool during the first process sequence of the adaptive CNC machining process. In the optimized specific machining process (see Figure 19), the blade LTE of and the four benchmark facets are machined in the first process sequence, and the position state of the machined benchmark facet is measured based on the on-machine measurement to record the blade benchmark facet position information.

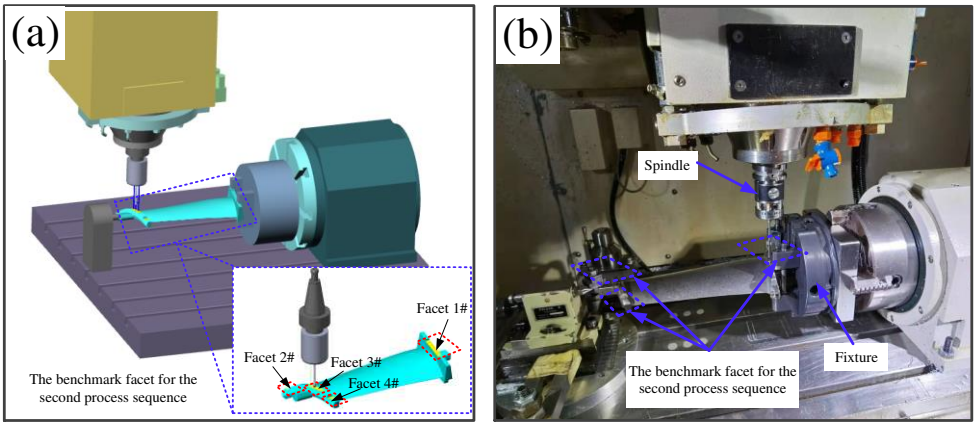


**Fig. 23** The benchmark facet for the second process sequence measurement in the four-axis machine tool in the first process sequence of the blade adaptive CNC machining process.

The second process sequence will be performed when obtains the machined blade LTE and the benchmark facet for the second process sequence measurement in the first process sequence. Figure 23 is the on-machine measurement of the second process sequence adaptive CNC machining process. The position status of the benchmark facets 1#, 2#, 3# and 4# (see Figure 23) on the four- axis machine tool (the first process sequence) and five- axis machine tool (the second process sequence) are respectively obtained by on-machine measurement. The same single-point deviation value is obtained under the two fixture installation positions by the adaptive CNC machining process (see Figure 3), and the multi-process machining error data flow control is realized.

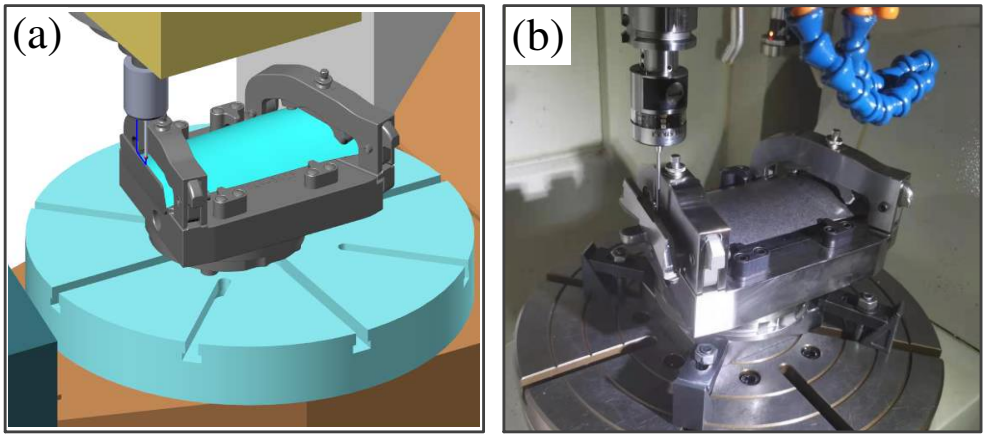


**Fig. 24** The machining benchmark facets on-machine measurement of the second process sequence of the blade adaptive CNC machining process.

The four benchmark facets for the second process sequence measurement are obtained by CNC machining process in a four-axis machine tool (see Figure 23) after

roughing machining, semi-finishing, finishing machining in the first process sequence and the adaptive adjustment in the five-axis machine tool of the second process sequence. Table 5 is the measurement value distribution of the multi-process collaborative machining benchmark conversion, and Figure 26 is the single-point deviation value of the corresponding machining benchmark facet.

**Table 5** Machining benchmark facets in the first and second process sequences

| Benchmark facets | Measurement points | The first process sequence | | | | The second process sequence |
|---|---|---|---|---|---|---|
| | | Under initial installation (mm) | Roughing milling (mm) | Remi-finishing milling (mm) | Finishing milling (mm) | After adaptive regulation (mm) |
| Facet 1# | 1 | 0.8423 | 0.8437 | 0.8443 | 0.8497 | 0.8502 |
| | 2 | 0.8423 | 0.8435 | 0.8439 | 0.8497 | 0.8476 |
| | 3 | 0.8417 | 0.8435 | 0.8437 | 0.8487 | 0.8471 |
| Facet 2# | 4 | 0.4487 | 0.2895 | 0.2903 | 0.2599 | 0.2836 |
| | 5 | 0.3707 | 0.3218 | 0.3224 | 0.2596 | 0.2785 |
| | 6 | 0.5237 | 0.5243 | 0.4037 | 0.2595 | 0.2793 |
| Facet 3# | 7 | 1.1189 | 1.1207 | 1.1215 | 1.1269 | 1.1242 |
| | 8 | 1.1188 | 1.1178 | 1.1184 | 1.1236 | 1.1218 |
| | 9 | 1.119 | 1.1197 | 1.1201 | 1.1255 | 1.1266 |

It can be seen from Figure 25 and Figure 26 that the single-point deviation value of the blade machining benchmark facets in the second process sequence is consistent with these values in the first sequence fixture installation state, and the second process sequence is in the five-axis machine tool fixture 1# installation state. The machining benchmarks transition from the first process sequence to the second process sequence is realized after two adaptive CNC machining process sequences, and this effect requires prerequisite of the sufficient stiffness of blade- fixture system.

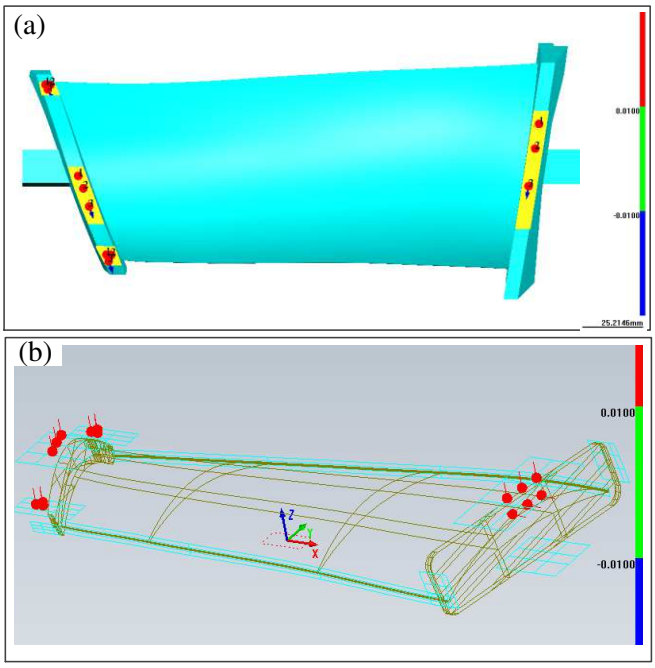


**Fig. 25** Machining benchmark facets measurement points, (a) in the first process sequence, (b) in the second process sequence

The above process scheme realizes the cohesion of two machining fixture benchmarks for the two process sequence, and the first process sequence is completed on the four-axis machine tool, which reduces the measurement time and cost than the adaptive CNC machining process scheme which still measures the blade body in the second process sequence.

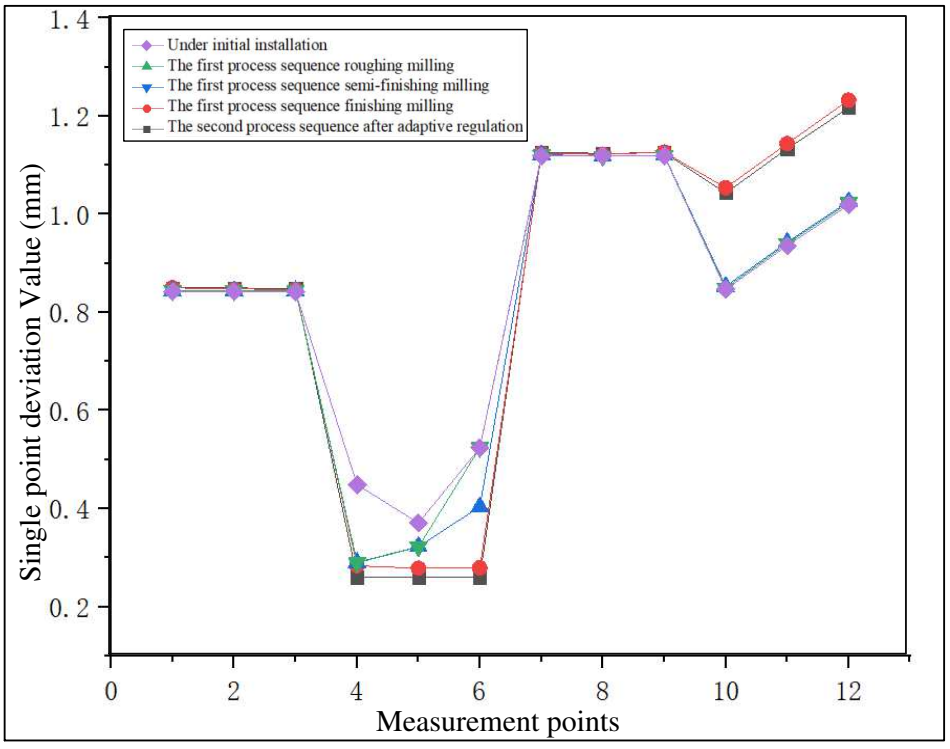

**Fig. 26** single- point deviation value change trend of blade machining benchmark facets in the first and second process sequence

## 4.4 Machining accuracy analysis of the optimized adaptive CNC machining process

Figure 27 is the single point deviation value of the blade body after the two process sequences of adaptive CNC machining process, it can be seen that the single-point deviation values of the blade body are uniformly distributed, and the single-point deviation values of all measurement points are more than 0mm. This is because that the blade body itself has a positive margin, and the positive margin value is about 0.008-0.05mm, and these deviation values still exist due to the blade body has not undergone subsequent CNC machining process. If these single-point deviation values are all greater than 0mm, and these single-point deviation values are evenly distributed, it can be indicated that the position of the blade does not deviate during the blade tenon root CNC machining processing, and this effect explains that the stiffness of the blade-fixture system is sufficient, which is consistent with the previous analysis of natural frequency and dynamic displacement response analysis.

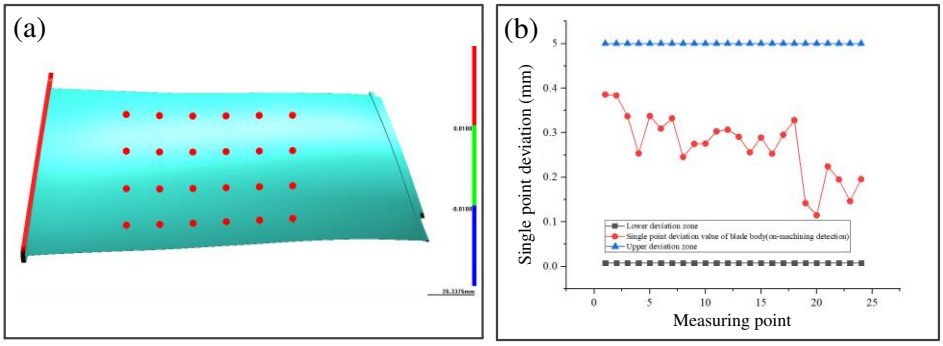


**Fig. 27** Single point deviation of blade body, (a) blade body measurement points, (b) single-point deviation distribution value of blade body.

Figure 28 is the single-point deviation value of the blade tenon root and tip after the two process sequences. It can be seen that the deviation values of all the measurement points are within the range of -0.007 to 0.007 mm, which shows that not only the machined surface profile meets the range of the machining error band, but also the position error of the blade tenon root and tip also meets the machining error range through the coordinated machining error data flow control of the two process sequences adaptive CNC machining process, which also shows that the stiffness of the blade-fixture system is sufficient, and the proposed adaptive CNC machining process

optimization based on machining error data flow control is feasible.

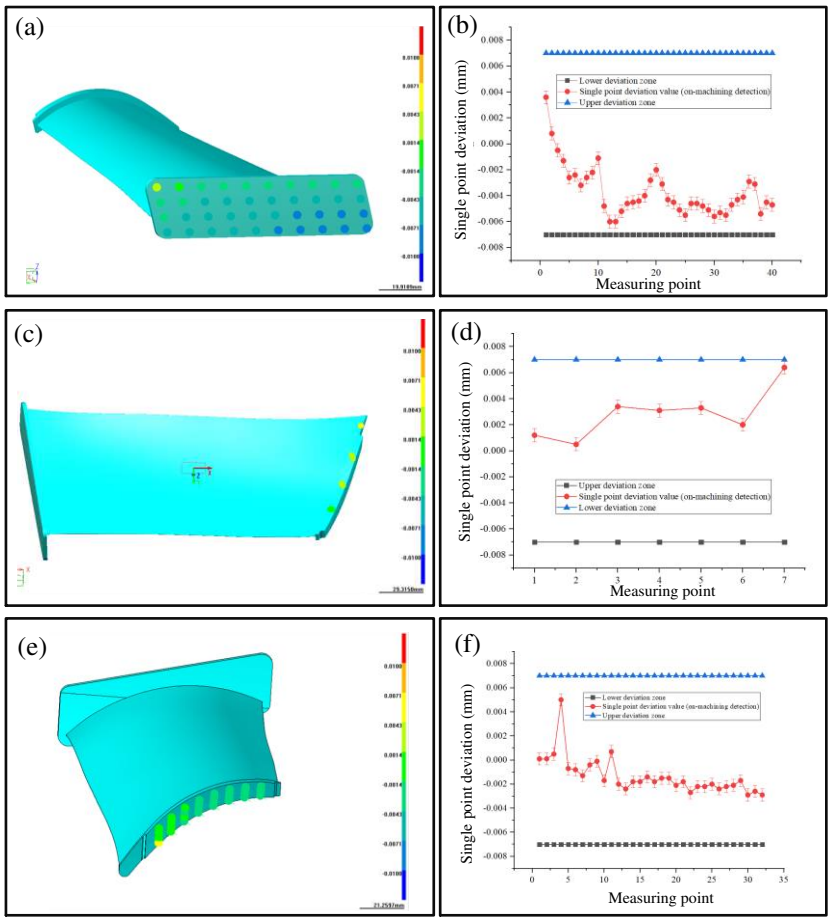


**Fig. 28** Single point deviation of blade tenon root and tip, (a) blade tenon root measurement points, (b) single-point deviation distribution value of blade tenon root, (c) blade tip measurement points, (d) single-point deviation distribution value of blade tip, (e) blade tip side measurement points, (f) single-point deviation distribution value of blade tip.

From the perspective of machining efficiency, the traditional low melting point alloy casting process has 15 CNC machining sequences (see Figure 2), while the optimized adaptive CNC machining process has only two CNC machining sequences (see Figure 19), and the number of CNC machining sequences is reduced by 87%. Compared with the twice on-machine measurement of the blade body profile points respectively for blade LET and the tenon root CNC machining process, the optimized adaptive CNC machining process only needs once blade body measurement and the measurement of the machining error transmission benchmark facets, and the number of measurement points on the benchmark facets are less than the measurement points on the blade body, and the number of measurement points is reduced by 50%, which

improves the efficiency by 50%.

The process chain of the optimized adaptive CNC machining process based on machining error data flow control is reduced by 87% compared with the low melting point alloy pouring process and 50% compared with adaptive CNC machining process of the twice on-machine measurement of the blade body. The reduction of blade process chain is beneficial to improve blade CNC machining efficiency.

In summary, the optimized adaptive CNC machining process based on machining error data flow control has the excellent performance in machining accuracy and efficiency.

# 5 Conclusion

In this study, the machining error data flow and dynamic displacement response of the multi- process adaptive CNC machining process of near- net- shaped blade are investigated by theoretical and experimental analysis, and the results can be summarized as follows:

1) The dynamic displacement response of the multi-process adaptive CNC machining process is controlled within 0.007mm, and the sufficient stiffness of blade-fixture system provides a prerequisite condition for adaptive CNC machining process optimization.

2) The optimized adaptive CNC machining process can realize the multi-process machining error control and high-precision manufacturing of near- net- shaped blade based on the multi-process data flow transmission control and sufficient stiffness of the multi-process blade- fixture system. The coordinated control of the two process procedures achieves the promotion of the machining accuracy of the blade

3) The process chain of the optimized adaptive CNC machining process based on machining error data flow control is reduced by 87% compared with the low melting point alloy pouring process and 50% compared with adaptive CNC machining process of the twice on-machine measurement of the blade body. The reduction of blade process chain is beneficial to improve blade CNC machining efficiency.

However, the proposed adaptive CNC machining process is based on the geometric adaptive processing technology, and the improvement of machining accuracy can be achieved under the premise of the sufficient stiffness of the blade- fixture system. How to achieve high-precision adaptive CNC machining process for the weak rigid process system will be the future research.

# 6 Declaration

## Acknowledgements

The author would like to acknowledge the support and contributions of our colleagues in Xi'an Aero-Engine (Group) Ltd. This research is supported in part by Xi'an Aero-Engine (Group) Ltd

## Funding

This research was supported in part by Xi'an Aero-Engine (Group) Ltd. and the National Natural Science Foundation of China [grant number 51575310].

## Availability of data and materials

The datasets supporting the conclusions of this article are included within the article.

## Authors' contributions

Dongbo Wu：experiment, data analysis, writing—review and editing
Hui Wang：methodology, formal analysis, original draft writing
Lei He: experiment
Jie Yu：experiment

## Competing interests

The authors declare no competing financial interests.

## Consent for publication

Not applicable

## Ethics approval and consent to participate

Not applicable

## References


1. Dongbo Wu, Hui Wang#, Jie Yu. Kaiyao Zhang, Machining fixture for adaptive CNC processing technology of near-net-shaped jet engine blade [J]. Chinese Journal of Aeronautics. 2020; 33, 1311- 1328.
2. Dongbo Wu, Hui Wang #, Kaiyao Zhang, Bing zhao. Research on adaptive CNC machining arithmetic and process for near-net-shaped jet engine blade [J]. Journal of Intelligent Manufacturing 2020; 31, 717- 744.
3. HU S J. Stream of Variation theory for automotive body assembly[J]. Annals of the CIRP, 1997, 46(1): 1-6.
4. Ceglarek D, SHI J, WU S M. A Knowledge-based diagnosis approach for the launch of the auto-body assembly process[J]. ASME Journal of Engineer for Industry, 1994, 116(4): 491-499.
5. Ceglarek D, SHI J. Fixture failure diagnosis for auto-body assembly using pattern recognition[J]. Journal of Engineering for Industry, 1996, 118: 55-66.
6. Walid Ghiea, Luc Laperriere, Alain Desrochers, Statistical tolerance analysis using the unified Jacobian–Torsor model, International Journal of Production Research, 2010, 48(15):4609-4630.
7. Yan Rong, Chen Wei, Peng Fangyu, Lin Sen, Li Bin, Closed-chain stiffness field modeling and stiffness performance analysis of multi-axis machining system [J]. Journal of Mechanical Engineering, 2012; 48 (1), 176-184.
8. Mantripragada Ramakrishna, Whitney Dani el E. Modeling and controlling variation propagation in mechanical assemblies using state transition models[J]. IEEE, Transactions on Robotic and Automation, 1999, 15(1): 124-140.
9. Jiayuan He, Yan Wang, Nabil Gindy. Pre-tensioning fixture development for machining of thin-walled components, Advanced Materials Research, 2011, (314-316):319-326.
10. James N. Asante, A combined contact elasticity and finite element-based model for contact load and pressure distribution calculation in a frictional workpiece-fixture system, International Journal of Advanced Manufacturing Technology, 2008, 39:578-588

11. Y. Wang, X. Chen, N. Gindy, Surface error decomposition for fixture development, International Journal of Advanced Manufacturing Technology, 2007, 31: 948–956
12. Y. Wang, X. Chen, N. Gindy, J. Xie. Elastic deformation of a fixture and turbine blades system based on finite element analysis, International Journal of Advanced Manufacturing Technology, 2008, 36:296-304
13. K.P. Padmanaban, K.P. Arulshri, G. Prabhakaran, Machining fixture layout design using ant colony algorithm based continuous optimization method, International Journal of Advanced Manufacturing Technology, 2009, 45:922-934
14. He Ning, Wang Zhigang, Jiang Chengyu, Zhang Bing, Finite element method analysis and control stratagem for machining deformation of thin-walled components, Journal of Materials Processing Technology, Volume 139, Issues 1–3, 20 August 2003, Pages 332–336
15. Weifang Chen, Lijun Ni, Jianbin Xue, Deformation control through fixture layout design and clamping force optimization, International Journal of Advanced Manufacturing Technology, 2008, 38:860-867
16. E. Budak, Analytical models for high performance milling. Part I: Cutting forces, structural deformations and tolerance integrity, International Journal of Machine Tools & Manufacture, 2006, (46):1478–1488
17. Baohai Wu, Ming Luo, and Dinghua Zhang, An efficient approach for identifying stable lobes with discretization method, Advances in Mechanical Engineering, 2013, doi:10.1155/2013/682684.
18. Ge Gao, Baohai Wu, Dinghua Zhang, Ming Luo. Mechanistic identification of cutting force coefficient in bull-nose milling process. Chinese Journal of Aeronautics, 2013, 26(3): 823-830.
19. Yilong Liu, Dinghua Zhang, Baohai Wu. An efficient full-discretization method for prediction of milling stability. International Journal of Machine Tools and Manufacture, 2012, 63:44-48.
20. Calleja, A, González, H, Polvorosa, R, Gómez, G., Ayesta, I., Barton, M. and de Lacalle, L.L., 2019. Blisk blades manufacturing technologies analysis. Procedia Manufacturing, 41, pp.714-722.
21. Calleja, A, Bo, P, González, H, Bartoň, M. and de Lacalle, L.N.L, 2018. Highly accurate 5-axis flank CNC machining with conical tools. The International Journal of Advanced Manufacturing Technology, 97(5), pp.1605-1615.
22. Zhang, Y, Chen, Z. and Zhu, Z, 2020. Adaptive machining framework for the

leading/trailing edge of near-net-shape integrated impeller. The International Journal of Advanced Manufacturing Technology, 107(9), pp.4221-4229.

23. Feng Yazhou. Construction of adaptive machining process geometry model for precision forged blades of aero-engine [D]. Northwestern Polytechnical University, 2018.
24. Tian Weijun. Research on the chatter suppression method for multi-axis machining of thin-walled blades [D]. Northwestern Polytechnical University, 2018.
25. Lu Yaoan. Research on tool path generation method for five-axis wide-row milling[D]. Shanghai Jiaotong University, 2017.
26. Lu, Y., Bi, Q. and Zhu, L., 2016. Five-axis flank milling of impellers: Optimal geometry of a conical tool considering stiffness and geometric constraints. Proceedings of the Institution of Mechanical
27. Liu Xuan. Research on adaptive machining model matching technology for hollow blades [D]. Nanjing University of Aeronautics and Astronautics, 2017.
28. Dongbo Wu, Bing Zhao, Hui Wang, Kaiyao Zhang, Jie Yu. Investigate on computer-aided fixture design and evaluation algorithm for near-net-shaped jet engine blades. Journal of Manufacturing Processes, 54 (2020) 393-412.